NGI

Applied Avalanche Research in Norway AARN

ANNUAL REPORT 2021

Neither the confidentiality nor the integrity of this document can be guaranteed following electronic transmission. The addressee should consider this risk and take full responsibility for use of this document.

This document shall not be used in parts, or for other purposes than the document was prepared for. The document shall not be copied, in parts or in whole, or be given to a third party without the owner's consent. No changes to the document shall be made without consent from NGI.

Ved elektronisk overføring kan ikke konfidensialiteten eller autentisiteten av dette dokumentet garanteres. Adressaten bør vurdere denne risikoen og ta fullt ansvar for bruk av dette dokumentet.

Dokumentet skal ikke benyttes i utdrag eller til andre formål enn det dokumentet omhandler. Dokumentet må ikke reproduseres eller leveres til tredjemann uten eiers samtykke. Dokumentet må ikke endres uten samtykke fra NGI.

Project

Project title:	Applied Avalanche Research in Norway (AARN)
Document title:	Annual Report 2021
Document no.:	20200017-03-R
Date:	2022-04-08
Revision no. /rev. date:	0 /

Client

Client:	NVE
Client contact person:	Odd Are Jensen and Aart Verhage
Contract reference:	Tildelingsbrev 04.12.2020

for NGI

Project manager:	Christian Jaedicke
Prepared by:	Peter Gauer, Sean Salazar, Kate Robinson, Dieter Issler, Regula Frauenfelder, Zhongqiang Liu, Christian Jaedicke, Graham Gilbert
Reviewed by:	Graham Gilbert, Christian Jaedicke, Dieter Issler

Summary

During the second year of the project period 2020-2022 of NGIs research project on snow avalanches, Applied Avalanche Research in Norway (AARN), work was conducted in all three work packages (WP 1 – Avalanche formation and release, WP 2 – Avalanche dynamics, WP 3 – Avalanche interaction) and several cross-package topics. The successful avalanche experiment in April 2021 has given us valuable insight into the dynamics of a large avalanche event and showed that the Ryggfonn test site produces the avalanches that are needed for the AARN research. During 2021, the results of the research activities have been published in peer-reviewed journals, summarised in technical notes, and presented online at national and international conferences and seminars. AARN personnel have been actively engaged in educational outreach activities, including as lecturers and student supervisors.

Contents

Review and reference page

1 Overview and administrative aspects

1.1 Project activities in 2021

Table 1 Summary of the AARN project activities in 2021. The research activities in most topics are ongoing.

WP 1 – Avalanche formation and release	• Simple model for variability of avalanche release areas
WP 2 – Avalanche dynamics	• Model for frontal entrainment • Outline of advanced snow avalanche model • Full-scale avalanche field test at Ryggfonn
WP 3 – Avalanche interaction	• Vulnerability functions for persons in buildings
Research infrastructure resources (RIR)	• New radar in Ryggfonn installed and tested • Preparation of historical Fonnbu data
Cross-Package Topics (CPT)	• Model for forest destruction by avalanches • Concept for quantitative risk assessment over extended areas • Continued documentation of interesting avalanche events

1.2 Involved personnel

The 22 individuals listed in Table 2 contributed to AARN activities in 2021.

Table 2 Contributors to AARN in 2021, listed alphabetically.

Researchers & scientific staff
Bozorgzadeh, Nezam
Frauenfelder, Regula
Gauer, Peter
Gilbert, Graham
Gisnås, Kjersti
Glimsdal, Sylfest
Issler, Dieter
Jaedicke, Christian
Kristensen, Krister
Langeland, Henrik
Liu, Zhongqiang
Robinson, Kate
Salazar, Sean
Sandersen, Frode
Strout, James Michael

Technical staff
Lied, Erik
Smebye, Helge Christian
Sverdrup-Thygeson, Kjetil

Administrative staff
Haaland, Kirsten Helness
Johnsen, Maren Kristine
Nakken, Robert
Raddum, Ellen

1.3 Budget

Table 3 gives an overview of the planned and actual allocation of resources to the different work packages. Deviations from the planned allocation are presented below.

Comments on the deviations from the planned allocation:

WP 0: In addition to general administration of AARN, budget use in WP 0 included several dissemination activities at conferences and the hiring of the post.doc candidate.

WP 1/WP 3: No significant budget deviations in WP 1 and WP 3.

WP 2: Additional resources were directed to WP 2 to conduct and analyse a full-scale field test at the Ryggfonn test site. Details below.

RIR: In addition to general maintenance, several infrastructure upgrades were completed at the Ryggfonn test site in 2021.

CPT: Several of the cross-package topics (CPT) are opportunistic and require that personnel can travel (e.g. for documentation of unique avalanche events). Other changes relate the availability of AARN personnel. Resources were redistributed to other activities.

Table 3 Budgeted allocation and actual use of resources per work package in 2021 (amounts in kNOK).

	WP 0 (Admin & reporting	WP 1	WP 2	WP 3	RIR	CPT	PostDoc	Total
Allocated	350	400	700	400	650	900	600	4 000
Used	591	434	1 493	381	500	401	0	3 800
Difference	-241	-34	-793	19	150	499	600	200

Dr. Callum Tregaskis started as a post-doctoral researcher in AARN on 1 November 2021. The position was delayed as the Dr. Tregaskis needed to complete his doctoral thesis prior starting at NGI. The first two months of this position (in 2021) have been financed by NGI. AARN will finance this position starting in 2022.

1.4   Dissemination

Peer-reviewed publications

Nishimura, K., Barpi, F., and <u>Issler, D.</u> (2021). Perspectives on snow avalanche dynamics research. *Geosciences* **11**, 57. DOI 10.3390/geosciences10110466.

Presentations at conferences, seminars and meetings

Gauer, P. (2021) Avalanche measurements at the Ryggfonn test site during the winter 2020/2021. Nordisk konferanse om snøskred og friluftsliv, Gol, 5.–7. November 2021.

Issler, D.: Towards an Improved Parameter-Free Entrainment Model for Snow Avalanches, EGU General Assembly 2021, online, 19–30 Apr 2021, EGU21-16564, https://doi.org/10.5194/egusphere-egu21-16564, 2021.

Jaedicke, C., Issler, D., Gleditsch Gisnås, K., Salazar, S., Robinson, K., Gauer, P., Langeland, H., Domaas, U., Liu, Z., Glimsdal, S., Sandersen, F., Mo, K., Frauenfelder, R., Heyerdahl, H., Breien, H., and Gilbert, G.: Recent advances in applied avalanche research in Norway, EGU General Assembly 2021, online, 19–30 Apr 2021, EGU21-11202, https://doi.org/10.5194/egusphere-egu21-11202, 2021.

Jaedicke, C., Mueller K. (2021). Teknisk – vitenskapelige snøskredfag på Norske Universiteter. Nordisk konferanse om snøskred og friluftsliv Gol, Norway, 5.–7. November 2021.

Robinson, K., Bozorgzadeh, N., Issler, D., and Liu, Z. (2021). What are the chances of surviving in a building hit by an avalanche? Nordisk konferanse om snøskred og friluftsliv Gol, Norway, 5.–7. November 2021.

Salazar, S., Paulsen, E.M., Emhjellen, L.A., Gauer, P., Frauenfelder, R., and Smebye, H.C. (2021). 3D modelling of an avalanche experiment using multi-platform remote observations. Virtual Geoscience Conference, September 2021.

Reports/Technical Notes

AARN Project Team. Annual report 2020. NGI Report 20200017-02-R.

Robinson, K., Liu, Z., and Issler, D. Vulnerability of structures and persons in buildings. NGI Technical Note 20200017-02-TN. Draft version from 2020/2021 will be revised, extended and published in 2022.

Issler, D. A simple model for the variability of release area size. NGI Technical Note 20200017-03-TN. Draft version from 2021 to be extended and published in 2022.

Gauer, P., Aalerud, A. H. and Body, N. S. Avalanche observations versus numerical avalanche model: Simple test of model performance. NGI Technical Note 20200017-04-TN.

Gauer, P. and Langeland, H. WP 2 – Full-scale experiments at Ryggfonn. Ryggfonn avalanche observations 2019/2020. NGI Technical Note 20200017-05-TN.

Gauer, P., Langeland, H., Salazar, S. and Kristensen, K. WP 2 – Full-scale experiments at Ryggfonn. Ryggfonn avalanche observations 2020/2021. NGI Technical Note 20200017-06-TN. Final version to be published in 2022.

Issler, D. Frontal entrainment in snow avalanches and other gravity mass flows. NGI Technical Note 20200017-08-TN. Draft version from 2021 will be extended and published in 2022.

Gauer, P. CPT 3 – Quantitative risk assessment. Remarks on the uncertainty in the delimitation of hazard zones based on historical observations. NGI Technical Note 20200017-09-TN. To be revised and published in 2022.

Patras, S., 2021. Analysis of two slushflows back simulated with RAMMS. Oslo, Norway.

1.5 Teaching and student supervision

Nilsen, Elise Øyberg (UiO, Dept. of Geosciences): *Implementation of the Norem–Irgens–Schieldrop model in two dimensions.* MSc thesis 2021–2022 co-supervised by A. Kääb and D. Issler. The student switched to another topic in June 2021.

Storebakken, Brage (UiO, Dept. of Geosciences): *The effect of forest on the snowcover in Nordmarka, Oslo*. MSc thesis 2021–2022 co-supervised by T. Schuler and D. Issler. Work ongoing, to be submitted in summer 2022.

Bélières-Frendo, Amaury (École Nationale Supérieure de Techniques Avancées –ENSTA Paris): *Implementation of simple entrainment models in a 1D avalanche model.* Internship during 2nd year of 2ème Cycle in engineering. Supervision by D. Issler. Due to the pandemic and travel restrictions, the student could not come to Norway and supervision was only by e-mail and video-conferencing.

Patras, Sophie (École Nationale Supérieure de Techniques Avancées –ENSTA Paris): *Analysis of two slushflows back simulated with RAMMS.* Internship during 2nd year of 2ème Cycle in engineering. Supervision by P. Gauer and C. Jaedicke. Due to the pandemic and travel restrictions, the student could not come to Norway and supervision was only by e-mail and video-conferencing.

UNIS AGF-212 (2021) Avalanche week. Taught by Christian Jaedicke

UiT GEO-3222 Snow avalanches – Science and Management, 10 ECT project course of three weeks. Taught by Christian Jaedicke

2 WP 1 – Avalanche formation and release

2.1 Variable size of release areas and volumes

The size of the release area plays an important role in the dynamics of snow avalanches, which is reflected in the strong volume dependence of the friction parameters recommended for use with the well-known Voellmy-type model RAMMS::-AVALANCHE (SLF, 2017). It has also been practical knowledge for a long time that the release area in a given path increases with the return period of the event; very frequent events may involve only a moderate fraction of the potential release area (PRA). This important property of snow avalanches has received surprisingly little attention in avalanche research (Maggioni & Gruber, 2003). In simulations for practical hazard mapping, the choice of release area is completely left to the intuition of the expert.

During tests of NAKSIN with nominal return periods between 10 and 100 years, unrealistically large endangered areas were predicted. This shortcoming could be traced directly to the size of the release areas, which NAKSIN so far assumes equal to the entire PRA. To improve this, a simple conceptual model has been developed that is compatible with the workflow and concepts of NAKSIN and efficient yet has a clear physical foundation. The model is described in (Issler D. , 2022) and will be briefly summarized here.

The NAKSIN module for release areas finds connected sets of grid cells satisfying several topographic criteria, chief among them the slope angle, which must be within a predetermined range. Each of the PRAs is characterized by its mean altitude, mean slope angle, and area. PRAs below a threshold area are discarded. In the module for release probability, the altitude is used for adjusting the gridded climate data from SeNorge, and the mean slope angle enters the formula for the factor of safety of an infinite uniform slope, which is tested for millions of synthetic situations created according to the weather statistics.

In the infinite-slope approximation used hitherto, the factor of safety decreases with increasing slope angle θ until $\theta = 45°$. Thus, if one considered only the steepest sub-areas, higher release probabilities would result. These sub-areas are kept from releasing by the forces transmitted, not along the weak layer but through the slab. The driving gravitational force on a slab limited to some area is proportional to the area and the slab depth. The stabilizing force along the weak layer is proportional to the area and the weak-layer shear strength, the one along the perimeter increases linearly with the slab depth and with the length of the perimeter, which grows as the square root of the area. Moreover, the strength is a weighted mean of shear, tensile and compressive strength of the snow forming the slab.

The proposed procedure consists of the following steps:

1. Find the largest connected sub-areas $\mathcal{B}_i$ of a given PRA $\mathcal{B}_0$ in which the slope angle exceeds a certain value θ_i, with $\theta_{i+1} > \theta_i$.
2. For each of the $\mathcal{B}_i$, find the area A_i, perimeter L_i, and mean slope angle $\psi_i > \theta_i$.

3. In each Monte Carlo trial, use a *finite-slope* stability criterion to determine which of the $\mathcal{B}_i$ first becomes unstable as snow accumulates under the given nivo-meteorological conditions of this trial. Record this index i and the corresponding fracture depth.

4. Count the avalanche releases for each $\mathcal{B}_i$ and extract the dependence of the release size on the return period. Similarly, the dependence of the fracture depth on the return period is obtained.

This model will be implemented and tested in 2022.

2.2 Effects of wind and weather on snowpack properties

The task has been replaced by other activities in 2021.

2.3 Simple probabilistic release models

See work described in Sec. 6.4 Forest effect.

3   WP 2 – Avalanche dynamics

3.1   New instrumentation for avalanche dynamics research

3.1.1   Use of drones in avalanche experiments

In 2021, drones continued to be used as observation and data gathering tools. Specifically, the April 11th avalanche experiment at Ryggfonn (described in Section 3.2) provided a unique opportunity to gather imagery by drone to support mapping of snow erosion, deposit and calculation of mass balance. An automated drone survey methodology, developed in Year 1 of AARN, was successfully deployed to map the lower portion of the avalanche path, both before and after the experiment, as well as in a snow-free condition (in summer). Additionally, a drone was used as a hovering camera in the valley to record video of the avalanche.

Digital snow surface models were constructed for geospatial analysis using a directly georeferenced Structure-from-Motion photogrammetry workflow to the combined total of 800 individual drone images. Total mobilized snow volume was estimated from the difference between the pair of independently georeferenced surface models (before, after the event, as depicted in Figure 1, Figure 2) while orthomosaics provided high-resolution overviews of the avalanche path (Figure 3, Figure 4). Furthermore, a pre-avalanche snow height map was produced based on a comparison with the snow-free terrain model.

Figure 1. Comparison of drone image-derived elevation models generated from pre- and post-avalanche images; deposition around the retaining dam. Scale in vertical meters.

5.0 m
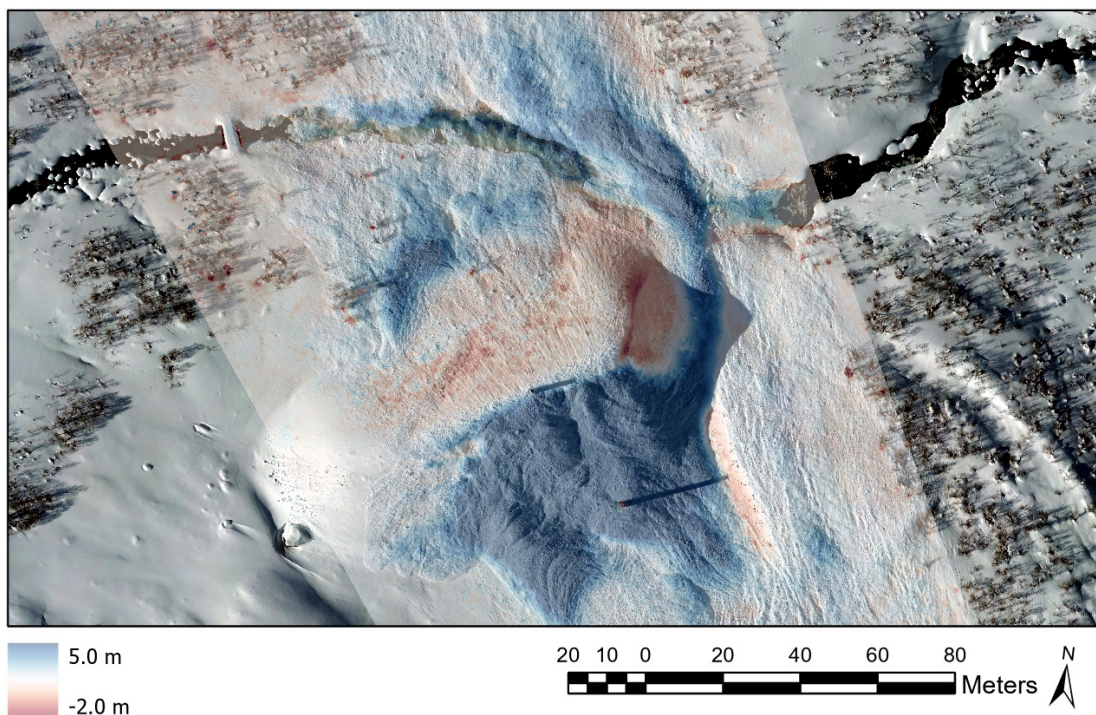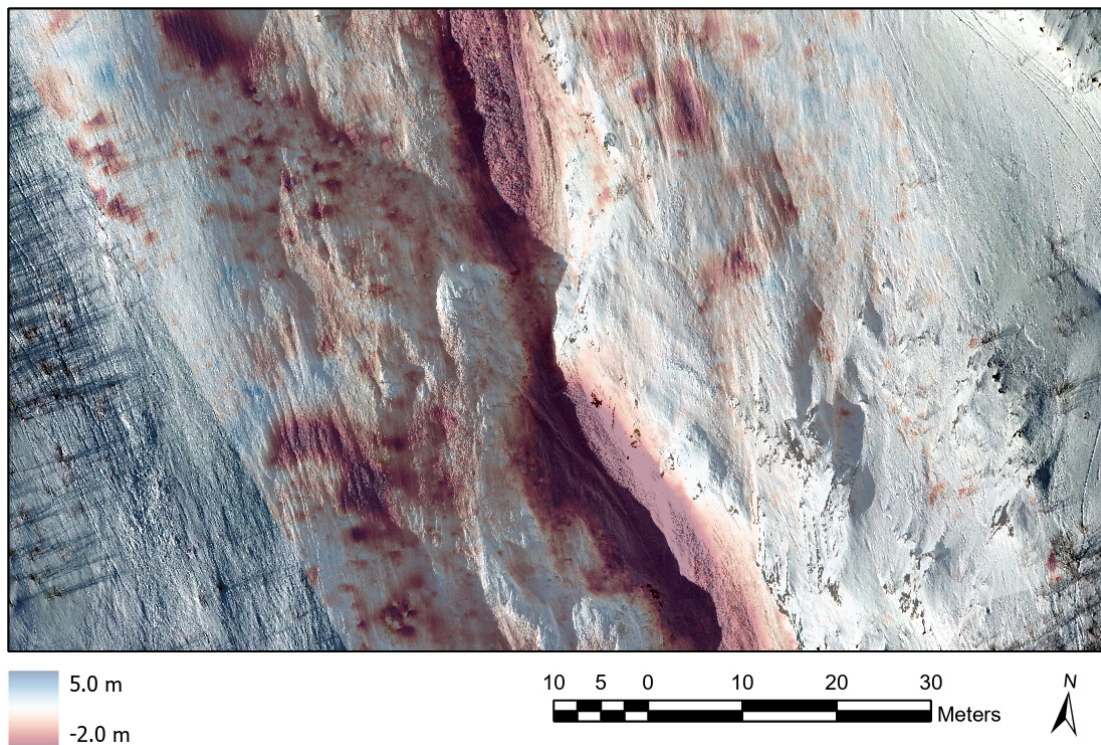
-2.0 m

10 5 0 10 20 30 Meters N

Figure 2. Comparison of drone image-derived elevation models generated from pre- and post-avalanche images; erosion areas along the avalanche path. Scale in vertical meters.
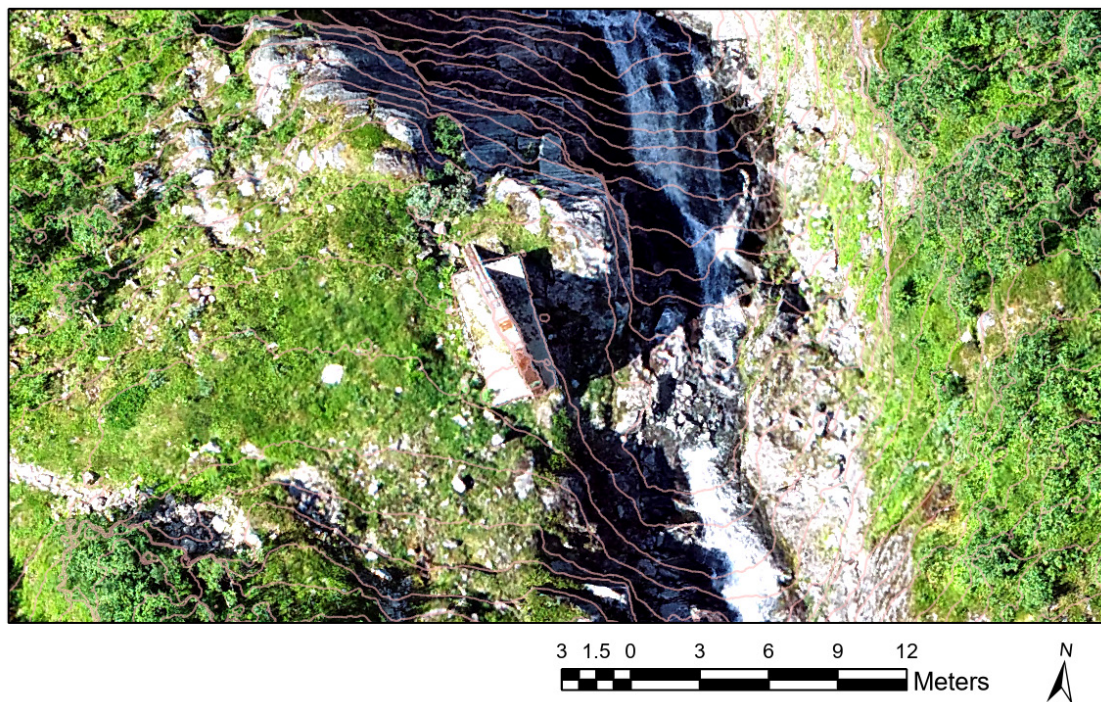

3 1.5 0 3 6 9 12 Meters N

Figure 3. Drone image-derived orthomosaic around the concrete wedge; snow-free imagery from 08.07.2021. Contour lines at 1 meter intervals.
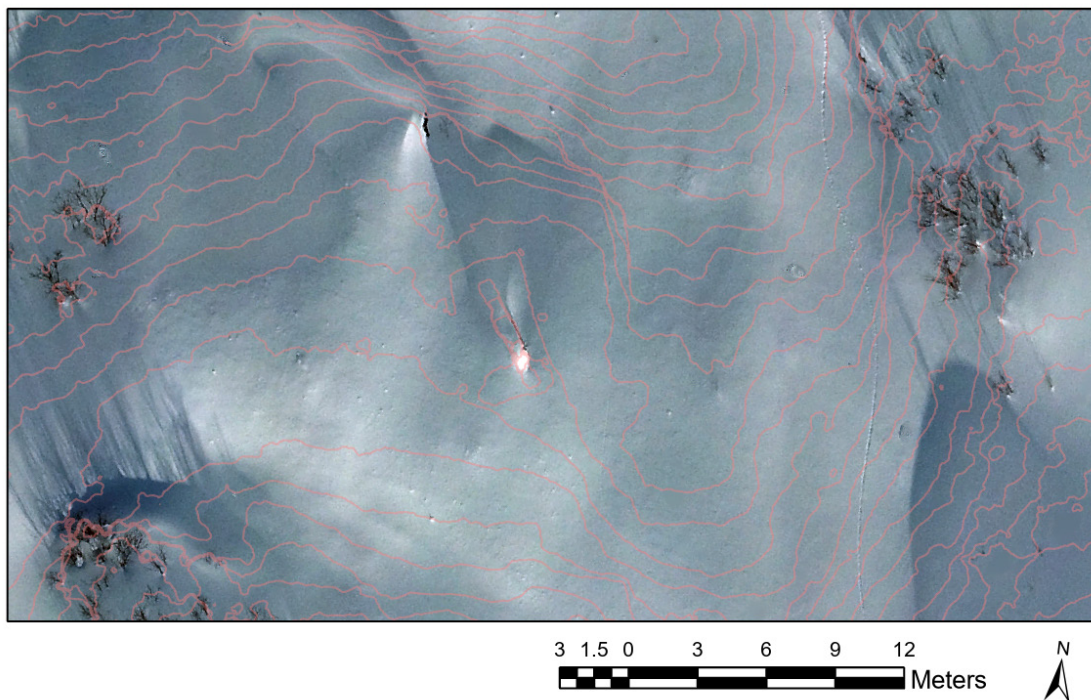
Figure 4. Drone image-derived orthomosaic around the concrete wedge prior to avalanche experiment on 11.04.2021 with contour lines from snow-free survey. Contour lines at 1 meter intervals.

3.1.2 Opportunities at small avalanche test sites

Besides full-scale experiments on large avalanches, there is a two-fold interest in carrying out full-scale experiments on small avalanches. For one, they are less costly and - to some degree - less difficult than measurements at a site like Ryggfonn. Also, it may be possible to carry out a larger number of measurements if mobile equipment can be used. Most importantly, detailed information on specific processes like entrainment, deposition and fluidization can be gathered by studying the avalanche deposits in detail.

In 2015, K. Nishimura (Nagoya University) initiated a research project to study the dynamics of small avalanches with a multitude of different measurement techniques. Niseko, a ski resort at the foot of a dormant volcano in southern Hokkaido, Japan appeared to be most suitable: large quantities of cold, dry snow in high winter, good facilities (public transport to Niseko, lodging, ski lifts, snowcats), good connections to knowledgeable ski patrols. Two small, easily accessible avalanche paths (lengths of 100–200 m) were selected; in one of them, the ski patrols are permitted to use explosives for avalanche control. There are no fixed installations except for seismic sensors near one of the paths. Video-filming in the visible and infra-red range as well as Doppler radar measurements can be carried out, however, from suitable and safe locations. D. Issler has participated in several campaigns, however, no avalanches could be released then. This failure is mainly due to the severe restrictions imposed by the resort managers: An artificial release was attempted only at the end of the last day of ski lift

operation, when the snow pack was completely humid and began to freeze again. At neither site was it allowed to close off a small terrain strip to maintain an undisturbed snow cover for the experiments.

The powdery high-winter snow for which Niseko is famous provides ideal conditions for testing a recently proposed yet untested hypothesis about fluidization of dry-snow avalanches by expulsion of pore air from the snow cover (see Section 3.5 for details). A mobile measurement panel was constructed at Hokkaido University, about 1×1 m^2 in size, aligned in the flow direction, and 5–10 cm wide towards the avalanche. On its one side, pairs of pressure sensors are installed at different heights, with one sensor measuring the total pressure and the other the pore pressure (the opening of the funnel leading to the pressure sensor itself is covered by a fine mesh that will keep snow particles out but allow the air pressure to propagate in). To obtain velocity information, a well-established technique is used that cross-correlates the signals from pairs of light-emitting diodes/photo cells mounted a few centimetres apart in the flow direction. So far, this measurement device has not been tested in an avalanche: Whenever the team succeeded in installing it before the experiment, no avalanche could be released; when an avalanche occurred spontaneously after the experiment, the measurement wall had been removed.

Different methods that could increase the chance of successful avalanche release without using explosives have been discussed, e.g., injection of water at the bottom of the snow cover or just above an impermeable layer (buried ice crust). A promising approach has been proposed by NGI, inspired by experiments carried out in Switzerland: Plastic sheets were placed in small slopes where one wished to prevent large snow masses from building up. Under suitable conditions (sufficiently steep slope, plastic sheets repelling water and thus preventing the snow from freezing to them), new snow would slide down in relatively small quantities. A similar approach can be used at Niseko at low cost, provided that the plastic sheets can be installed shortly before an anticipated snowfall and the area surrounding the sheets closed off for skiers.

The original project terminated in 2019 but a new five-year project under the leadership of NIED's Snow and Ice Research Centre (SIRC) in Nagaoka has been started. Due to the COVID-19 pandemic, no experiments could be carried out in 2021 and 2022, but it is expected that a new attempt will be possible in the winter 2023. In preparation for this, NGI will discuss possible improvements of the release methods and measurement techniques with our colleagues at SIRC and the BfW Innsbruck team, who also wish to participate. One of the options that should be explored is to use the measurement wall in the surroundings of Innsbruck, where the chances of successful release with explosives are higher and a simple foundation for fixing the wall in the ground could likely be built. To this end, it is planned to carefully investigate different options in a Technical Note in 2022.

3.2   Avalanche experiments at Ryggfonn

Eight natural avalanches of size 2 to 3 (on the EAWS avalanche size scale) occurred during the winter 2020/2021. The avalanches released mid-February, during the second half of March, in the beginning of April, and early May. For some of the avalanche events, pressure data and/or rough estimates of local velocities, were collected. An autonomous Doppler radar system, installed in the fall of 2020, provided first velocity data for some of the events. Although field observations were carried out on few occasions after an event, the gained information was limited by weather constraints. In addition to measurements of natural releases, a field campaign was launched on April 11th, 2021 resulting in a successful full-scale experiment. The released avalanche was of relative size R4 (EAWS size 4). A brief overview of the collected raw data and a preliminary analysis can be found in (Gauer, Langeland, Salazar, & Kristensen, 2022).

3.3   Reasons for extreme avalanche runouts

There are many observations of avalanches attaining extraordinarily long run-out under special conditions. In avalanche hazard mapping, where the Norwegian regulations demand that events with a return period of 100, 1000 or even 5000 years be considered, such so-called "dragon kings" are of great importance. To our knowledge, long run-out is always connected to a high degree of fluidization of a substantial fraction of the avalanching mass. Earlier work (Issler and Gauer, 2008; Issler, 2017) suggests that there may be three physical mechanisms that together cause fluidization: (i) Air flow over the avalanche head produces under-pressure and tends to suspend small snow particles from the avalanche surface, forming a powder-snow cloud. (ii) Vigorous collisions between snow particles creates dispersive pressure that reduces the flow density and the shear stress at a given shear rate, thus allowing higher shear rates and higher velocities, which favour longer run-out. (iii) Air is pressed out of the snow cover under the load of the avalanche flowing over it. As it flows upward through the avalanche, the pressure gradient supports a large fraction of the avalanche weight, reducing both the friction and the density (Issler D. , 2017).

Constructing a complete and realistic model that incorporates at least the mechanisms (ii) and (iii) will require refinement of the equations describing the compressibility of the snow cover and the permeability of the avalanche. This work had to be postponed in 2021 and will be taken up again in 2022. As a first step towards a complete numerical model, we intend to implement the mechanism (ii) described in (Issler & Gauer, Exploring the significance of the fluidized flow regimes for avalanche hazard mapping, 2008) in a simple 1D flow model and thereafter add equations for the generation and dissipation of excess pore pressure (mechanism iii). A simple 1D model with Voellmy friction law has been developed from a Matlab/Octave code courtesy of Dr. Chris Johnson, University of Manchester during an internship (see Sec. 1.5), but some stability problems in the modified code must be resolved first. (The same code will also be used in the work summarized in Secs. 3.4 and 3.5.)

3.4   Entrainment and deposition models

In this activity, the focus in 2021 was on improving the frontal entrainment model due to Eglit, Grigorian and Yakimov, hereafter called EGYEM. This model is doubly remarkable because it was part of the very first continuum avalanche model (Grigorian, Eglit, & Yakimov, 1967) and is consistently closed, i.e., it does not contain freely adjustable parameters that are not determined by the material properties of the snow. This is in sharp contrast with most entrainment models proposed later, which are to a large degree empirical and often have questionable physical justification. Later entrainment modelling efforts both in Russia and in the West have focused on basal entrainment, but frontal entrainment is of relevance in wet-snow avalanches, where it can be observed directly. Chute experiments have also provided insight into this process (Barbolini, Biancardi, Cappabianca, Natale, & Pagliardi, 2005).
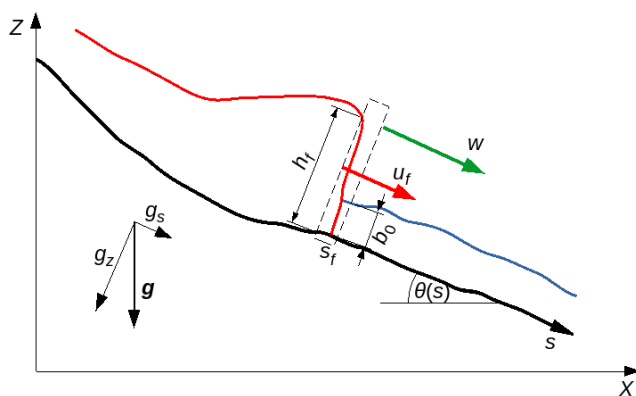

Figure 5. Schematic representation of the first continuum avalanche model and its treatment of frontal ploughing as a shock. Blue line – snow cover, red line – avalanche, green arrow –front propagatioon velocity. From (Issler D. , 2022)

The EGYEM simplifies the frontal entrainment region to a moving shock, i.e., a discontinuity of density, flow depth and velocity. Then, conservation of mass and momentum across the shock determine the propagation velocity of the shock, which in turn determines the entrainment rate. The EGYEM makes the important simplifying assumption that the entire erodible snow cover (typically, the new-snow layer) of depth $b_0(s)$ is entrained, provided the hydrostatic pressure force that the avalanche front exerts on the erodbible snow layer exceeds the resistance of the latter. Where this is not the case, three possible outcomes are proposed by Eglit (1983): (a) The avalanche front stops (and possibly resumes motion and entrainment once enough mass from behind has accumulated to increase the pressure force beyond the threshold). (b) The avalanche flows over the snow cover without eroding it. (c) The avalanche erodes the snow cover only to the depth that makes the pressure force equal to the resistance force. However, no criteria are given for choosing one of these modes in a given situation. Moreover, closer scrutiny showed that the formula given for case (c) leads to zero front propagation velocity.
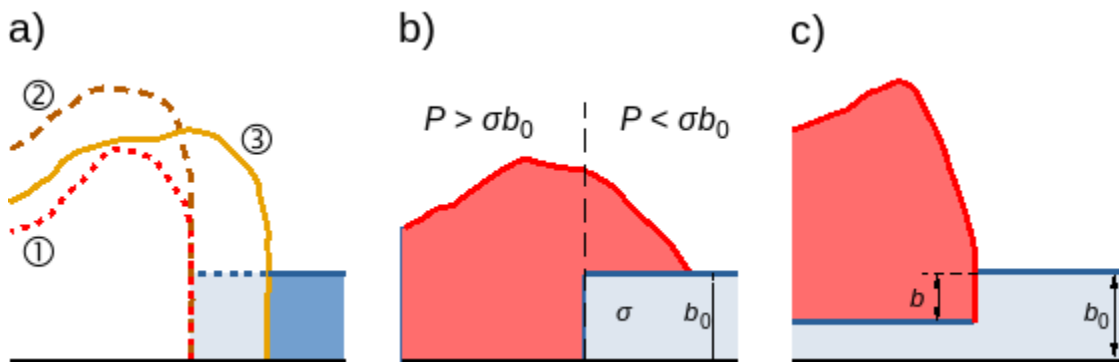
Figure 6. Schematic representation of the three possible types of front behaviour if the hydrostatic pressure force from the avalanche (red) is smaller than the resistance force from the snow cover (blue). a) Avalanche stops ① until enough snow has piled up ② to overcome the resistance ③. b) Avalanche flows above snow cover without entrainment. c) Partial entrainment. From (Issler D. , 2022)

The assumption of full-depth entrainment appears difficult to justify on mechanical grounds. Reanalysis of the shock equations (internship of A. Bélières-Frendo, see Sec. 1.5) seemed to allow a solution that determines both the front propagation velocity w and the entrainment depth $b \leq b_0$, but inconsistencies were encountered. It finally turned out that the boundary conditions at the moving shock front were not formulated correctly - at the shock front, sub-critical inflow conditions prevail. Accordingly, one of the two conditions imposed by mass and momentum conservation provides the one boundary condition required in this situation. The other condition allows to find w, but only if the entrainment depth b is known. Lacking further physical conditions, $b = b_0$ is the only natural and non-trivial choice.

In the course of further work, it has been recognized that also the total energy must be conserved across the shock and that this may provide a third condition, which can be used to determine $b \leq b_0$ dynamically. The preliminary results are presented in (Issler D. , 2022); this document will be updated when the jump condition for the total energy has been formulated and a formula for the entrainment depth derived.

3.5   Mathematical equations of an improved avalanche model

In preparation for the development work by the AARN post-doc (C. Tregaskis), we analysed the requirements on a future advanced avalanche model with regard to hazard mapping, design of protection measures like catching and deflecting dams, and dimensioning of buildings exposed to avalanche impacts. All use cases will benefit greatly from a model that accounts for the dense, fluidized and suspension flow regimes. Past experience also points at the need for physically realistic modelling of entrainment and deposition. In hazard mapping and the design of protection measures, a depth-averaged (quasi-3D) model offers the best compromise between physical realism, simulation detail, speed, and ease of use. A model including the powder-snow cloud would remedy an important shortcoming in NAKSIN, NGI's code for generating

avalanche hazard indication maps. However, code efficiency is of paramount importance in this use case. When dimensioning buildings with complicated geometries, a full 3D model is needed, but such projects represent at most 1% of NGI's or other consulting companies' projects. In such cases, a commercial, all-purpose Computational Fluid Dynamics code may provide an adequate approach.

Based on these considerations, a possible set of equations for a three-layer quasi-3D model has been outlined. The erodible snow cover forms the lowest layer. Besides the Exner equation (mass balance), an equation describing compaction under an external load (due to the avalanche) is needed to characterize this layer (see Sec. 0). The second layer describes the dense and medium-dense components of the avalanche, with a density that can vary in space and time to describe the transition between flow regimes. Excess pore pressure due to the escaping interstitial air in the snow cover plays an important role in this layer, and its evolution must be modelled. The snow particles typically range from grain size to football size. In contrast, the third layer (suspension layer) contains only fine snow grains that are held in suspension by the turbulence of the air. At this stage, it is an open question whether closures based on averaged quantities are sufficient or the turbulence needs to be modelled explicitly in the suspension layer.

The minimum system will consist of two partial differential equations (PDEs) for the snow cover (mass balance and density), four PDEs for the dense/fluidized layer (mass and momentum balance, excess pore pressure), and four PDEs for the suspension layer (mass, momentum and volume or density). Compared to a Voellmy-type model (four PDEs), we expect the computation times to be about three times as long. This is acceptable for all envisaged applications, including NAKSIN and quantitative risk assessment (see Sec. 6.3). The main challenge will be to develop suitable constitutive equations to describe the rheology of the two moving layers and all mass exchange terms between the layers.

These questions will be studied intensively in 2022. In parallel, extensions to this equation set and alternative approaches based on segregation will be investigated. Among the most interesting extensions are an explicit equation for the balance of turbulent kinetic energy in the suspension layer, akin to the four-equation variant of the Parker–Fukushima–Pantin model of turbidity currents (Parker, Fukushima, & Pantin, 1986), and an extra equation for the location of the centre-of-mass of the suspension layer (Kowalski & McElwaine, 2013) to obtain information on the vertical profiles of density, velocity and pressure, which are important in practical applications.

4 WP 3 – Avalanche interaction

4.1 Alternative mitigation measures

A major shortcoming in avalanche protection structures in Norway has been recognized in recent years: Many if not most of the catching dams have been dimensioned based on too low velocity estimates. This is compounded by the predominance of dams with relatively gently inclined upstream sides, which are now known as much less efficient than steep sides. In most cases, enlarging the dams is not feasible due to lack of space or geotechnical constraints.

Experience from the full-scale test site Ryggfonn, which features a 16 m high dam, suggests that such earth dams often can stop wet-snow avalanches or the dense part of dry-snow avalanches but not their much faster fluidized part. The latter is characterized by its density and, hence, impact pressure being much lower than in the densest part of the flow. This opens the possibility of mitigating the hazard by other means than building a higher dam.

In Japan and Austria, a few semi-permeable structures have been built to reduce the mass and speed of avalanches that cannot be stopped either due to their low density and large flow height ("powder-snow avalanches") or because the topographic conditions are difficult (Figure 7). The idea behind the steel structure near Maseguchi (left panel) is that it will affect the largest (and most energetic) turbulence elements most, triggering an energy cascade to smaller turbulence elements. This will enhance sedimentation from the dilute flow and thus reduce pressure and run-out distance.

Figure 7. Semi-permeable structures for braking fast, large avalanches. Left: Steel structure near Maseguchi, Nagaoka Prefecture, Japan against powder-snow avalanches. Right: Large concrete structure in Austria. Images courtesy S. Margreth, SLF Davos.

At a much smaller scale, the effect of modified rockfall nets on small-to-medium size snow avalanches has been tested in recent years with some success, again in Austria (Figure 8). Here, the objective was to stop the avalanche mass partly or entirely. Tests have shown that nets with openings of diameter d will retain almost the entire flow mass if sufficiently many particles have diameter $d/2$ or larger.

Figure 8. Steel nets for stopping a small avalanche in Austria. Image taken from the producer's website (https://www.rud.com/en/products/barriertech/avalanche-protection.html)

These experiences suggest that catching dams that are high enough to stop the dense core of avalanches could also be effective against the fast, fluidized part of the avalanche if one installed nets of suitable height and mesh size on the crown of the dam. Depending on the circumstances (avalanche speed, available storage volume, mechanical strength of the earth dam), one may choose the mesh size to retain most of the fluidized part or to let most of the mass through to avoid back-filling and/or damaging loads on the nets.

There is presently not enough knowledge and experience for discerning whether nets on existing dams indeed are technically feasible and effective at reasonable cost. However, given that this is the only realistic-looking proposal for upgrading conventional earth dams to fulfil their original purpose, it deserves further study. If the personnel resources permit, the following questions will be studied in 2022:

- How can one test and demonstrate the effectiveness of semi-permeable barriers against fast, fluidized or suspended avalanche flows? Can one scale up laboratory experiments with enough confidence to justify construction of such dams?
- Can one give simple yet reliable rules for choosing the preferred mesh size and for dimensioning the forces?

Answering these questions will likely necessitate experimental work with a scale model and collaboration with partners outside NGI.

4.2 Vulnerability of structures and persons in buildings

4.2.1 Avalanche database

In 2021 work continued updating and expanding the database of historical avalanche events in Norway which impacted buildings when people were present inside.

For each avalanche event, the database contains information on the number of people who were present in the building at the time of the avalanche, and the number of people who survived or died. In addition, the degree of damage to each building was assessed based on the damage scale presented in (Issler, Jónsson, Gauer, & Domaas, 2016) and shown in Table 4. The degree of damage assessments completed in 2021 were done considering an overall value for the entire building, and not considering where (e.g. which floor) people were in the building. A total of 425 individuals in 78 separate buildings were considered from the database for statistical modelling, discussed in the next section.

Table 4 Characterization of different degrees of damage to a building due to an avalanche impact.

Degree of damage D	Damage description
Category 1: 0–10%	All spaces intact to slightly skewed. Big voids and structure are stable.
Category 2: 10–40%	Impact side partly pushed in or skewed, limited voids at impact side, big voids at lee side, partly skewed/damaged internal walls. Snow/avalanche debris in at least 10 – 20% of the building.
Category 3: 40–70%	Impact side pushed in/collapsed, big voids approx. 50%, small voids due to snow avalanche debris approx. 20%. Snow/avalanche debris in at least 50% of the building.
Category 4: 70–90%	Impact side pushed in/collapsed, internal walls collapsed, no big voids, small voids due to snow avalanche debris approx. 20%. Snow/avalanche debris in at least 90% of the building.
Category 5: 90–100%	All spaces destroyed, (almost) no voids remain, large part of the building scattered, most walls destroyed.

In many cases the degree of damage to the buildings varies by floor and there is information in the data base allowing this to be characterized. Furthermore, location of the people inside the building is known more specifically, such as on which floor or in some cases in which room. Therefore, it is possible to perform per-floor assessments to obtain a more accurate assessment of degree of building damage leading to survival or fatality. Work on separating damage on a per-floor basis is ongoing and will be completed in 2022.

4.2.2   Statistical modelling

The Bayesian framework was adopted for analysing the data. Two statistical models were formulated. First, a simple logistic[1] regression model was fitted to the data:

$$\text{Pr(survival)} = \text{logit}^{-1}(\beta_0 + \beta_{damage} \times damage) \tag{1}$$

where probability of survival is modelled as a liner function of degree of damage on the logit scale. The best fit curve and 95% credible interval from this model are shown in Figure 9 (blue thinner set of curves). Note that this model assumes that, given the degree of damage, the probability of survival is the same for all buildings. The raw estimates of per-building probability of survival are also shown on the figure with (green) "×" symbols. A visual assessment suffices for concluding that the logistic regression reasonably captures probability of failure of aggregate data (i.e. average of probability of survival for a given degree of damage, shown as filled circles) but fails to capture the between-building variability exhibited by the data, shown as green "×" symbols.

To address the above-mentioned shortcoming of the simple logistic regression model, a more flexible two-level model is assumed. First, given the degree of damage, each building is assumed to have its own probability of survival; simultaneously, the probabilities of survival are assumed to have arisen from a common population distribution with a mean modelled as a linear function of degree of damage (on the logit scale) and with common residual standard deviation σ:

$$\text{Pr(survival)} = \text{logit}^{-1}(\beta_0 + \beta_{damage} \times damage + \varepsilon) \tag{2.a}$$

$$\varepsilon \sim \text{Normal}(0, \sigma) \tag{3.b}$$

Such multi-level models are also known as hierarchical models. Note that the model in Eq. (1) assumes *identical* probability of survival conditional on degree of damage while the hierarchical model of Eq. (*2*) assumes the probabilities of survival are *similar but not identical* (formally, *exchangeable*; see e.g. (Lunn, Jackson, Best, Thomas, & Spiegelhalter, 2013) for more details). The fitted hierarchical model is summarized as the (red) thicker set of curves on Figure 9. Visually, and relative to the results of the logistic regression model, the hierarchical model predicts (on average) higher/lower probability of survival for lower/higher degrees of damage. Also, the 95% predictive interval contains most of the observed data (although not 95%). Furthermore, preliminary quantitative model comparison using leave-one-out cross-validation suggests that the hierarchical model provides a better fit to the data. However, this evidence is not taken as decisive yet because the data base is being improved. See section 4.2.3 for the intended improvements to the data base and the statistical models.

---

[1] The *logistic* function maps the probability space [i.e. the range (0,1)] to $(-\infty, \infty)$: $\text{logit}(x) = \log\left(\frac{x}{1-x}\right)$. The inverse logistic function maps back to the unit scale: $\text{logit}^{-1}(x) = \frac{e^x}{1+e^x}$.
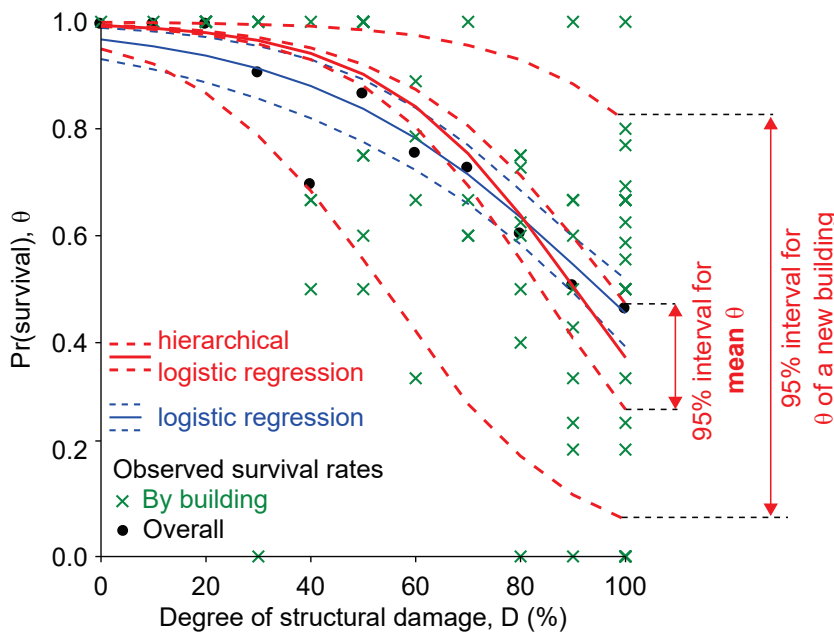
Figure 9. Regression models for predicting probability of survival

4.2.3   Future work

Avalanche database

The database will be continued to be updated in 2022, specifically focusing on the following:

- ⌐ Breaking down the damage assessments on a per-floor basis, where possible
- ⌐ Assigning uncertainty values to individual damage assessments
- ⌐ Obtaining damage assessments and corresponding uncertainty values from multiple individuals
- ⌐ Inclusion of international avalanche events

As discussed in section 4.2.1, work has already begun on separating the damage assessments down to a per-floor basis, to obtain a more accurate representation of survivability of a person based on the damage to the building where that person was located.

All damage assessments in the current statistical models are taken as 100% confident, i.e. they do not contain any assessment of uncertainty. Work began in 2021 to assess a subjective likely interval (say, 95% probability) on individual damage assessments, to be included in the statistical models. This will be completed in 2022, and new models fitted.

To date, the damage assessments are all based on the judgment of one individual. In 2022 the plan is to obtain assessments from several other individuals, to gain some understanding of the between-assessor variations. This is particularly important because the degree of damage is the only predictor in the model and is being assessed subjectively based on incomplete qualitative information.

Finally, it is desirable to explore data from international avalanche databases, at least to check the predictive accuracy of the Norwegian wood framed building model on international data and decide if the model is transferrable.

Statistical modelling

The current models will be re-fitted to the per-floor data. The models will also be extended to include the uncertainty in degree of damage assessment from one individual, and further for combining assessments from multiple individuals.

Structural vulnerability

The second portion of the assessment of vulnerability of people inside of buildings hit by avalanches is to assess the degree of damage to the building based on a design avalanche (i.e. an avalanche with reasonable intensity values for areas where buildings are present. The intensity value could be defined as flow height, pressure, etc.). To accomplish this, we plan to numerically simulate the degree of damage of a building impacted by an avalanche with specified parameters and repeat with several building types and a range of avalanches.

The input information required for the numerical model includes selection of one or more typical buildings (i.e. Norwegian wood-frame buildings with for example one or two floors, or with different orientations to the avalanche impact), and selection of desired avalanche parameters to impose on the building (e.g. flow height and pressure). The model should provide sufficiently detailed output to allow assessment of the degree of damage according to the scale presented in Table 4, which is then used to determine the survivability potential for each avalanche.

4.3   Residual risk

4.3.1   Consequences of constructing properly dimensioned buildings in exposed areas

The guidelines to §7-3, 2nd clause in the Technical Regulations in TEK17 open for the possibility of construction in potentially endangered areas, provided the buildings are dimensioned to withstand the expected forces from an avalanche with the maximum return period T relevant for the building category in question. It is expected that scarcity of suitable safe construction areas in many municipalities, in conjunction with new and more economical high-strength construction techniques (particularly, cross-laminated timber), will lead to increased use of such areas.

While the buildings tolerate the maximum pressures from the design avalanche, there is a (nominal) annual probability $1/T$ for an avalanche exceeding the design pressure. Depending on how much the pressure exceeds the design pressure, the building will take damage and its inhabitants are at risk of being severely injured or killed. While the *individual* probability for injury or death is well below $1/T$, the *societal* risk will increase considerably if the number of exposed persons increases strongly. This issue should

therefore be considered carefully at an early stage of land-use planning—before detailed planning of new construction areas is initiated.

There is thus urgent need for quantitative risk assessment (QRA) in such cases, see Sec. 6.3 for the research and development plans. Here we summarize the elements of such an analysis and the corresponding data requirements to emphasize that this is a demanding cross-disciplinary problem.

- First, the *hazard* must be determined. This can be phrased as the need to estimate the probability distribution function (PDF) of the impact pressure at each potential building location. This goes beyond standard run-out calculations with a topographic-statistical or simple dynamical run-out model: many calculations with different initial conditions and friction parameters following suitable PDFs must be carried out and their results converted into location-specific PDFs for impact pressure.
- Second, the degree of building damage must be estimated from the PDF of impact pressure. This requires that the response of a representative building to a wide range of loads be analysed (by means of Finite-Element calculations).
- Third, the PDFs of building damage must be combined with empirically determined vulnerability functions for persons in buildings (Secs. 4.2.1 and 4.2.2) and the expected exposure numbers to obtain the residual societal risk.
- Fourth, when it comes to deciding whether the augmented risk is acceptable or not, one may need to weigh it against the expected gain in terms of keeping peripheral settlements alive, increasing economic opportunities, etc.

Depending on the progress made in Task 3.2 on the vulnerability of persons and buildings and in CPT 3 on improved tools for QRA, a case study is envisaged, possibly involving the municipalities of Stryn and/or Ørsta.

4.3.2 Uncertainty in the delimitation of hazard zones based on historical observations.

Based on an idealised example, we studied the influence of the inherent temporal and spatial fuzziness of observations and their influence on the delimitation of hazard zones.

The calculations performed suggest that the estimates of expected return periods solely based on historical observations as input for the hazard zoning should be regarded as being within an order of magnitude, even when the calculations are based on well documented events. This interpretation was already made by Mears in 1992. An overly detailed delimitation of avalanche hazard zones boundaries based on these estimates can be counterproductive because it can give a false impression of accuracy.

The above remark is in many aspects also valid for many of modelling approaches. This suggests that the derived nominal probabilities should also be regarded as being within an order of magnitude rather than an exact value.

4.3.3 Avalanche/protection structure interaction

It is rarely possible to design a protection structure (e.g., a catching dam) that will stop all avalanches at all times. Some avalanches might overflow protection structure and flow downstream. One way of quantifying the residual risk related to overflow is to estimate the avalanche runout shortening caused by the protection structure. An avalanche/dam interaction law has been studied by a few researchers, e.g. Faug et al. 2003, 2008.

5 Research infrastructure resources (RIR)

AARN utilises two main sites with actively deployed research infrastructure; (1) the full-scale test-site Ryggfonn and (2) the mountain research station Fonnbu. Both are organised as a "leiested" and receive basic funding from AARN to maintain the resources and provide services for the research activities.

5.1 Full-scale avalanche test-site Ryggfonn

Under this task, necessary repairs and updating of the data acquisition system at the Ryggfonn avalanche test site (Stryn municipality, Vestland county, western Norway) were carried out in preparation for the 2021/22 winter season. The updates included a snow height sensor for the weather station, positioned at the Grasdalen valley bottom. Moreover, the autonomous pulsed Doppler radar was replaced to improve stability of the data collection. The first radar was installed in early 2021 in cooperation with BFW (Innsbruck, Austria).

The 2021 experiment in Ryggfonn has shown the shortcoming of some sensors in the experimental setup. NGI and the AARN team is working on possible solutions for the issue and we might use some of the forthcoming budget to finance these improvements.

5.2 Research station Fonnbu

The research station Fonnbu has been in high activity in 2021. The station has been used by the Norwegian Armed Forces for course activities, by the AARN project for the Ryggfonn experiment, collection of weather data and the documentation of the snow and avalanche situation in the Grasdalen valley. Pictures from the newly installed automated camera are used in other NGI funded projects for development and testing of automated algorithms for avalanche relevant information such as snow surface changes, avalanches and new snow amount. The SKnow project used the station for field campaigns and continuous radar observations of the snow pack. The H2020 project MEWS uses both Ryggfonn and Fonnbu as base for the testing of IOT instrumentation in the rough and challenging mountain environment. Efforts are taken to provide 5G cover in the valley to support these activities.

6 Cross-package topics (CPTs)

6.1 Climate and climate change

The effect of climate change on the avalanche climate in Norway has been discussed in several spin off projects like KlimaVei and NordicLink based on the knowledge, data and experience from AARN. Work is ongoing to gather and streamline historical data from the old manual and partly automated weather data from Fonnbu. Once ready, this data will be made available for the public.

6.2 Avalanche observations and monitoring

Important new and historical avalanche events are constantly registered in the NGI database. The database follows the national database design and focuses on the technical and details of events as well as possible documentation of damages and effects of the avalanche. Data is regularly exchanged with the national database.

6.3 Quantitative risk assessment

Three separate lines of avalanche research in AARN and other NGI projects in recent years provide the foundation for developing a methodology and numerical tools for quantitative risk assessment (QRA) by combining them in a suitable way: a simple model for release probabilities (AARN, see Sec.6.4; NAKSIN), an efficient code for obtaining the spatial distribution of run-out probability (from a recent internal research project), and work on extracting vulnerability functions for persons in buildings and for buildings impacted by avalanches (AARN, see Sec. 0). In 2021, shortage of personnel resources allowed only to sketch the conceptual framework and to outline the corresponding tools. If time permits in 2022, the concept will be refined and described in detail, and a prototype code will be developed. A brief outline of the conceptual framework is given here.

$$\boldsymbol{T}^i = \sum_{n=1}^{N} \begin{pmatrix} V_n D_n(p_n^i) \\ E_n L\left(D_n\left(p_{n_n}^{\ i}\right)\right) \end{pmatrix}, \tag{4}$$

As summarized in Sec. 4.3.1, many factors determine the total risk due to avalanches (or other natural hazards) in a given area. Assume there to be N objects $\mathcal{O}_n$, $n = 1, ..., N$ at risk at their locations $\boldsymbol{x}_n$. Each of the objects has its value V_n and vulnerability $D_n(p)$ in the range $[0,1]$. We suppose that the *intensity* of an event can be quantified satisfactorily in terms of the maximum avalanche pressure at the location of the object. For simplicity, we presently also assume the vulnerability to be expressed in terms of the degree of damage as defined by Issler et al. (2016) and that the monetary loss due to an event can be approximated as $T_n = V_n D_n(p)$. Furthermore, let the exposure of persons at the locations $\boldsymbol{x}_n$ be given as numbers E_n, which can take values larger than or equal to 0, with $E_n = H_n$ if there are permanently H persons in the building $\mathcal{O}_n$, etc. As in Sec.0, it is furthermore assumed that a universal lethality function for persons in buildings, $L(D)$,

in terms of the degree of damage is valid and known. Then the expected loss T in an event i affecting the N objects $\mathcal{O}_n$ with pressures p_n^i can be expressed as an abstract vector where the upper row accounts for the material losses (building value including furniture and the inhabitants' valuables) and the lower row represents the number of severely injured or killed persons.

The expression is a conditional expectation value, i.e., it quantifies the loss *if* an event occurs with the intensities p_n at the locations of the objects. To obtain the total expected loss per year, one must sum over all possible events, weighted by their probabilities. Thus, we need the probability distribution functions (PDFs) for the pressure at the locations x_n, $P_n(p)$, where $P_n(p)\mathrm{d}p$ is the annual probability of a peak pressure in the range $[p, p+\mathrm{d}p]$ occurring at x_n. Then one obtains

$$T = \sum_{n=1}^{N} \int_0^\infty \begin{pmatrix} V_n D_n(p) \\ E_n L\big(D_n(p)\big) \end{pmatrix} P_n(p)\mathrm{d}p \,, \tag{4}$$

The next step is to estimate the PDFs $P_n(p)$,. To keep the discussion simple, we assume here that only one avalanche path threatens the study area. If we know its release area, the (annual) PDFs for the release depth, d_0, the shear strength of the erodible snow cover, τ_c, and the friction parameters μ and k, then we can simulate a large number of avalanche events with the initial and boundary conditions following the mentioned PDFs. For each simulation, one records the maximum pressure at the locations x_n. Step-wise approximations of the sought PDFs of pressure, $P_n(p)$, follow directly from the ordered lists of recorded pressures. If desired, they can be fitted to a suitable function.

To complete the task, we must find the PDFs of d_0, τ_c, μ and k. A simple stability model combined with experimentally obtained relations between different snow-cover properties like density and shear strength the code voellmy-pro, which was developed at NGI a few years ago. It is based on the

- ⌐ We anticipate that the following development steps will be necessary to obtain a practically usable code for QRA:NAKSIN must be modified so as to record fracture depths, weak-layer shear strengths, snow densities and mean temperatures of all events so that the (cumulative) PDFs of these quantities can be tabulated.
- ⌐ The correlations between temperature, weak-layer shear strength, and the friction parameters must be estimated so that appropriate PDFs of τ_c, μ and k can be constructed. Most likely, their mean values will be found to vary deterministically with the temperature but to fluctuate around this value according to some PDF.
- ⌐ Instead of calling MoT-Voellmy for the run-out calculation, NAKSIN shall invoke Voellmy-pro and furnish the (cumulative) PDFs of d_0, τ_c, μ and k.
- ⌐ Voellmy-pro must be modified to record, for each run-out calculation, the maximum pressure at the locations x_n. When the pressure values are sorted for each object location, the lists can be transformed into the PDFs of pressure, $P_n(p)$.

⌐ An extension of NAKSIN or a separate program is needed to evaluate Eq. (4). To this end, the object values V_n, human exposure E_n, the building vulnerability, $D_n(p)$ and the lethality function $L(D)$ must be provided as input.

6.4   Forest effects

The work on a simple probabilistic release model for avalanche hazard mapping (Gauer, 2018), was continued with the main focus on improving the forest parameterization based on literature data. The model involves meteorological data from SeNorge, such as HS, HNW, RR, SWE, TA. The model now includes an extended forest parametrization that also accounts for interception. Forest influences the snowpack and its stability in various way. Forest covers to a certain degree the amount of snow on the ground. Loading intensity is reduced due to interception, which depends on the leaf area index (LAI), the crown cover, and the amount of precipitation; with increasing precipitation the effect of interception decreases. The forest cover also influences the weak-layer properties directly, and it is generally agreed that the spatial extent of weak layers decreases with increasing crown cover. In certain case, "tree bombs" can however cause intense loading of the snowpack and so lead to avalanche release.

Once an avalanche has been released, forest stands will exert a certain braking effect on the flow. If the forest is not too dense, the deflection of the flow around one tree will not appreciably influence the flow around a neighbouring tree. The braking effect can then be approximated as a contribution to the bed shear stress that is proportional to n, the number of trees per unit area and their average area exposed to the flow, i.e., the mean diameter, D, times the flow depth, h. Laboratory experiments and numerical simulations of granular flows allow to express the drag created by the trees in terms of contributions $\Delta\mu$ and Δk to the friction and drag coefficients of a Voellmy-type model, the resistance term of which then becomes $\tau_b = (\mu + \Delta\mu)\rho g \cos\theta + (k + \Delta k)\rho u^2$. This was implemented in NGI's in-house code MoT-Voellmy several years ago, with $\Delta\mu \approx \frac{5}{4}nDh$ and $\Delta k \approx \frac{1}{2}nDh$.

Comparison of simulations disregarding the braking effect of forest with simulations using new high-quality forest data (data set SR16-beta produced by NIBIO) over extended areas has since revealed that the braking effect is clearly overestimated in densely forested areas. This might be a shortcoming of the formulation of the braking term, but another possibility is that the avalanche quickly destroys the forest, upon which much of the retarding effect disappears.

To test this hypothesis, a simple extension of the model implemented in MoT-Voellmy has been devised: At each timestep and for each computational cell, the bending moment the avalanche exerts on the trees is calculated and compared to the bending resistance of the trees. The latter depends on the wood quality, quantified by the so-called modulus of rupture (MoR, about 50 MPa for beech trees) and the diameter of the tree. Alternatively, a tree can be uprooted if the soil is soft or the root system not wide and deep enough. Once the bending moment exceeds the bending resistance, the cell is

flagged, and the stand density reduced exponentially with time as $n_{ij}(t + \Delta t) = n_{ij}(t)[1 - \lambda(D)\Delta t]$. The decay constant λ depends on the average time a tree needs to fall, which increases considerably with the tree diameter; for simplicity, inverse proportionality between the decay constant and the mean tree diameter is assumed.

We lack specific measurements to verify the model. Nevertheless, comparisons of simulations without forest, with "indestructible" forest and with forest being destroyed gave encouraging results. One test case was an idealized "hockey stick" slope, the other a known avalanche path from the Melshorn, municipality of Volda (Figure 10).

Figure 10. Comparison of simulations of an avalanche from the Melshorn, municipality of Volda. Green area is reached by the avalanche assuming the forest cannot be destroyed. The red area shows the run-out if the braking effect of the forest is ignored. The blue area results if the trees are destroyed once their bending strength is exceeded by the avalanche [NaturAct].

6.5 Dissemination

Researchers and experts from the AARN project have participated in a large number of for a, seminars, conferences and in media where results from the AARN project are conveyed to the public. Activities were limited by the corona pandemic and will be intensified in 2022.

7 Related projects and partnerships

The knowledge- and infrastructure base in AARN is used in several other projects that work with different aspects of snow, avalanches and risk mitigation.

7.1 Ongoing R&D projects

7.1.1 KlimaVei

The project studies the possibilities and preconditions for including the effects of climate change in socioeconomic analysis that are the basis for investment decisions in large infrastructure projects in Norway. NGIs contribution to the project is competency on climate and natural hazards in general and avalanches in specialisation. The project is a cooperation with the national road administration, Vestlandsforskningen, Nye Veier and Menon and is financed by the Norwegian Research Council.

7.1.2 GEOSFAIR

GEOSFAIR investigates and tests the use of instrumented for faster and better assessments of landslide and avalanche danger in relation to roads and other liniar infrastructure. Drones can easily approach difficult terrain and transport light weight instruments that can help the specialists to gather information from areas that are not accessible for them. NGIs contribution to the project is snow and avalanche knowledge for the gathering of ground truth for verification of the drone data. The project is cooperation with the national road administration and SINTEF and is financed by the Norwegian Research Council. Link to the project web site.

7.1.3 NordicLink

NordicLink (2020-2023; financed by NordForsk) is a collaborative research project between NGI (project manager), Chalmers University of Technology (Sweden), the Finnish Metrological Institute, and infrastructure stakeholders in Norway (Statens vegvesen, Nye Veier AS, and BaneNor), Sweden, and Finland. The objective of NordicLink is to advance natural hazards research to secure Nordic linear infrastructure networks against climate induced natural hazards. Past and ongoing research activities and infrastructure in AARN are foundational to NGIs participation in this project. Synergies between NordicLink and AARN include activities on physically based

avalanche models, climate adaptive hazard and risk assessments, and sustainable solutions for avalanche hazard mitigation. Link to project webpage.

7.1.4   GEOMME

The GEOMME partnership for climate-induced geohazards mitigation, management, and education includes universities, research institutes, and municipalities in Norway (NGI, UiT, & Aurland kommune) Japan, and South Korea. Experiments, modelling, and assessment of snow avalanches are central topics in the project. Ryggfonn will be used for activities with the international partners in Norway. GEOMME is running from autumn 2021 until 2026 and is managed by NGI. The partnership is financed by the Norwegian Research Council. The partnership will increase the international presence of Norwegian snow avalanche research and the dissemination of practical outcomes to the municipal sector in Norway.

7.1.5   SKnow

The use of radar technology for the identification of dangerous a snowpack is the aim of the SKnow project. NGIs contribution is machine learning tools for radar signal analysis, snow sciences and avalanche knowledge. The project is in cooperation with ThinkOutside and SINTEF and is partly financed by the Norwegian Research Council.

7.1.6   MEWS – Eurostars

The MEWS project aims at developing a distributed, scalable and cost-effective mass movement early warning system. The project uses Ryggfonn as a demonstration area for the concept and has installed a number of low cost IOT instruments in the area. The project is financed within the H2020 EU program.

8   Project plan and budget – 2022

8.1   Revised work plan 2022

Table 5 Summary of the AARN project activities planned in 2022, based on the project proposal. Note the research activities in most topics are ongoing.

WP 1 – Avalanche formation and release	• Implementation and testing of model for variable release sizes • Workflow to quantify the probability distribution functions for release volumes and events for dynamic avalanche models • MSc thesis on snow cover in forest stands
WP 2 – Avalanche dynamics	• Further work on entrainment models • Fluidization model implemented numerically • Refined system of equations for mixed-avalanche model, and implementation in a multi-layer block model • Technical Note on experimental techniques at small test sites (if time permits)
WP 3 – Avalanche interaction	• Analysis of database on persons in buildings hit by avalanches • Technical Note on wire nets on top of catching dams (if time permits), as part of task on alternative mitigation measures
Research infrastructure resources (RIR)	• Seasonal maintenance and upkeep of the research infra-structure • Several field campaigns planned as part of AARN and in associated R&D projects
Cross-Package Topics (CPT)	• Technical Note on extending NAKSIN for task on quantitative risk assessment • Documentation of unique avalanche events arising during the 2022 snow season

8.2   Budget 2022

The Budget for 2022 is adjusted based on the experience of the last year and the have employed a PostDoc for 2022.

Table 6 Budgeted allocation for 2022 (amounts in kNOK)

	WP 0 (Admin & reporting)	PostDoc	WP 1	WP 2	WP 3	RIR	CPT	Total
Allocated	350	1 190	400	700	400	550	410	4 000

9   References

Barbolini, M., Biancardi, A., Cappabianca, F., Natale, L., & Pagliardi, M. (2005). Laboratory study of erosion processes in snow avalanches. *Cold Regions Science and Technology, 43*(1–2), 1–9. doi:10.1016/j.coldregions.2005.01.007

Eglit, M. E. (1983). Some mathematical models of snow avalanches. In M. Shahinpoor, *Advances in the Mechanics and the Flow of Granular Materials* (pp. 577–588). Clausthal-Zellerfeld, Germany: Trans Tech Publications.

Gauer, P. (2018). Avalanche probability: slab release and the effect of forest cover. *Proc. Intl. Snow Science Workshop 2018, Innsbruck, Austria* (pp. 76–83). Innsbruck, Austria: International Snow Science Workshop.

Gauer, P., & Kristensen, K. (2022). *Remarks on the uncertainty in the delimitation of hazard zones based on historical observations.* Oslo, Norway: NGI.

Gauer, P., Langeland, H., Salazar, S., & Kristensen, K. (2022). *WP 2 – Full-scale experiments at Ryggfonn. Ryggfonn avalanche observations 2020/2021.* Oslo, Norway: NGI.

Grigorian, S. S., Eglit, M. E., & Yakimov, Y. L. (1967). Novaya formulirovka i reshenie zadachi o dvizhenii snezhnoi lavini [A new formulation and solution of the problem of the motion of a snow avalanche]. *Tr. Vysokogorn. Geofiz. Inst., 12*, 104–113.

Issler, D. (2017). *Notes on fluidization of snow avalanches by air expulsion from the snow cover.* Oslo, Norway: NGI.

Issler, D. (2022). *A simple model for the variability of release area size.* NGI Technical Note 20200017-03-TN, Norwegian Geotechnical Institute, Oslo, Norway.

Issler, D. (2022). *Frontal entrainment in snow avalanches and other gravity mass flows.* NGI Technical Note 20200017-08-TN, Norwegian Geotechnical Institute, Oslo, Norway.

Issler, D., & Gauer, P. (2008). Exploring the significance of the fluidized flow regimes for avalanche hazard mapping. *Annals of Glaciology, 49*, 193–198. doi:10.3189/172756408787814997

Issler, D., Jónsson, Á., Gauer, P., & Domaas, U. (2016). Vulnerability of houses and persons under avalanche impact – the avalanche at Longyearbyen on 2015-12-19. *International Snow Science Workshop* (pp. 371–378). Breckenridge, Colorado: International Snow Science Workshop. Retrieved from http://arc.lib.montana.edu/snow-science/objects/ISSW16_O16.03.pdf

Kowalski, J., & McElwaine, J. N. (2013). Shallow two-component gravity driven flows with vertical variation. *Journal of Fluid Mechanics, 714*, 434–462. doi:10.1017/jfm.2012.489

Lunn, D., Jackson, C., Best, N., Thomas, A., & Spiegelhalter, D. (2013). *The BUGS Book. A Practical Introduction to Bayesian Analysis.* London, UK: Chapman Hall.

Maggioni, M., & Gruber, U. (2003). The influence of topographic parameters on avalanche release dimension and frequency. *Cold Regions Science and Technology, 37*, 407–419. doi:10.1016/S0165-232X(03)00080-6

Parker, G., Fukushima, Y., & Pantin, H. M. (1986). Self-accelerating turbidity currents. *Journal of Fluid Mechanics, 171*, 145–181. doi:10.1017/S0022112086001404

SLF. (2017). *RAMMS::AVALANCHE User Manual.* Davos, Switzerland: WSL Institute for Snow and Avalanche Research SLF.

Dokumentinformasjon/*Document information*

Dokumenttittel/*Document title*	Dokumentnr./*Document no.*
Annual Report 2020	20200017-03-R

Dokumenttype/*Type of document*	Oppdragsgiver/*Client*	Dato/*Date*
Rapport / Report	NVE	2022-04-08

Rettigheter til dokumentet iht kontrakt/ *Proprietary rights to the document according to contract*	Rev.nr.&dato/*Rev.no.&date*
Oppdragsgiver / Client	0 /

Distribusjon/*Distribution*
ÅPEN: Skal tilgjengeliggjøres i åpent arkiv (BRAGE) / OPEN: To be published in open archives (BRAGE)

Emneord/*Keywords*
Avalanche, research, snow, SP4

Stedfesting/*Geographical information*

Land, fylke/*Country*	Havområde/*Offshore area*
Norway	

Kommune/*Municipality*	Feltnavn/*Field name*
Stryn	

Sted/*Location*	Sted/*Location*
Strynefjellet	

Kartblad/*Map*	Felt, blokknr./*Field, Block No.*

UTM-koordinater/*UTM-coordinates* Zone: East: North:	Koordinater/*Coordinates* Projection, datum: East: North:

Dokumentkontroll/*Document control*
Kvalitetssikring i henhold til/*Quality assurance according to NS-EN ISO9001*

Rev/ *Rev.*	Revisjonsgrunnlag/*Reason for revision*	Egenkontroll av/ *Self review by:*	Sidemanns-kontroll av/ *Colleague review by:*	Uavhengig kontroll av/ *Independent review by:*	Tverrfaglig kontroll av/ *Interdisciplinary review by:*
0	Original document	2022-04-07 Christian Jaedicke	2022-04-07 Graham Gilbert		

Dokument godkjent for utsendelse/ *Document approved for release*	Dato/*Date*	Prosjektleder/*Project Manager*
	8 April 2022	Christian Jaedicke

2015-10-16, 043 n/e, rev.03

p:\2020\00\20200017\wp0 - project admin\delivery-result\reports\20200017-03-r_annual report 2021\20200017-03-r_annual_report_2021_final.docx

NGI (Norwegian Geotechnical Institute) is a leading international centre for research and consulting within the geosciences. NGI develops optimum solutions for society and offers expertise on the behaviour of soil, rock and snow and their interaction with the natural and built environment.

NGI works within the following sectors: Offshore energy – Building, Construction and Transportation – Natural Hazards – Environmental Engineering.

NGI is a private foundation with office and laboratories in Oslo, a branch office in Trondheim and daughter companies in Houston, Texas, USA and in Perth, Western Australia

www.ngi.no

NGI (Norges Geotekniske Institutt) er et internasjonalt ledende senter for forskning og rådgivning innen ingeniørrelaterte geofag. Vi tilbyr ekspertise om jord, berg og snø og deres påvirkning på miljøet, konstruksjoner og anlegg, og hvordan jord og berg kan benyttes som byggegrunn og byggemateriale.

Vi arbeider i følgende markeder: Offshore energi – Bygg, anlegg og samferdsel – Naturfare – Miljøteknologi.

NGI er en privat næringsdrivende stiftelse med kontor og laboratorier i Oslo, avdelingskontor i Trondheim og datterselskaper i Houston, Texas, USA og i Perth, Western Australia.

www.ngi.no

NGI

OSLO
TRONDHEIM
HOUSTON
PERTH